Bile Acids Trigger GLP-1 Release Predominantly by Accessing Basolaterally Located G Protein–Coupled Bile Acid Receptors

Cheryl A. Brighton,* Juraj Rievaj,* Rune E. Kuhre, Leslie L. Glass, Kristina Schoonjans, Jens J. Holst, Fiona M. Gribble,* and Frank Reimann*

University of Cambridge (C.A.B., J.R., L.L.G., F.M.G., F.R.), Metabolic Research Laboratories and Medical Research Council Metabolic Diseases Unit, Wellcome Trust-Medical Research Council Institute of Metabolic Science, Addenbrooke's Hospital, Cambridge CB2 0QQ, United Kingdom; Novo Nordisk Foundation Center for Basic Metabolic Research and Department of Biomedical Sciences (R.E.K., J.J.H.), the Panum Institute, University of Copenhagen, Copenhagen, Denmark; and Institute of Bioengineering (K.S.), School of Life Sciences, Ecole Polytechnique Fédérale de Lausanne, Lausanne CH-1015, Switzerland

Bile acids are well-recognized stimuli of glucagon-like peptide-1 (GLP-1) secretion. This action has been attributed to activation of the G protein–coupled bile acid receptor GPBAR1 (TGR5), although other potential bile acid sensors include the nuclear farnesoid receptor and the apical sodium-coupled bile acid transporter ASBT. The aim of this study was to identify pathways important for GLP-1 release and to determine whether bile acids target their receptors on GLP-1–secreting L-cells from the apical or basolateral compartment. Using transgenic mice expressing fluorescent sensors specifically in L-cells, we observed that taurodeoxycholate (TDCA) and taurolithocholate (TLCA) increased intracellular cAMP and Ca^{2+}. In primary intestinal cultures, TDCA was a more potent GLP-1 secretagogue than taurocholate (TCA) and TLCA, correlating with a stronger Ca^{2+} response to TDCA. Using small-volume Ussing chambers optimized for measuring GLP-1 secretion, we found that both a GPBAR1 agonist and TDCA stimulated GLP-1 release better when applied from the basolateral than from the luminal direction and that luminal TDCA was ineffective when intestinal tissue was pretreated with an ASBT inhibitor. ASBT inhibition had no significant effect in nonpolarized primary cultures. Studies in the perfused rat gut confirmed that vascularly administered TDCA was more effective than luminal TDCA. Intestinal primary cultures and Ussing chamber–mounted tissues from GPBAR1-knockout mice did not secrete GLP-1 in response to either TLCA or TDCA. We conclude that the action of bile acids on GLP-1 secretion is predominantly mediated by GPBAR1 located on the basolateral L-cell membrane, suggesting that stimulation of gut hormone secretion may include postabsorptive mechanisms. **(*Endocrinology* 156: 3961–3970, 2015)**

Gut hormones play key roles in the control of nutrient metabolism and are relevant for the treatment of type 2 diabetes and obesity (1). In particular, glucagon-like peptide-1 (GLP-1) promotes insulin release and lowers glucagon secretion from the pancreas and also inhibits food intake and gastrointestinal motility (2). GLP-1 is released from enteroendocrine L-cells, which comprise upto ~1% of intestinal epithelial cells. They are scattered along the intestinal tract, increasing in density toward the distal small intestine and colon. These open-type cells make di-

ISSN Print 0013-7227 ISSN Online 1945-7170
Printed in USA

Received April 10, 2015. Accepted August 12, 2015.
First Published Online August 17, 2015

* C.A.B. and J.R. contributed equally to the study and are joint first authors. F.M.G. and F.R. contributed equally to the study.

Abbreviations: ASBT, apical sodium-dependent bile acid transporter; BBS, bombesin; BSA, bovine serum albumin; CFP, cyan fluorescent protein; DMSO, dimethyl sulfoxide; FACS, fluorescence-activated cell sorting; FXR, farnesoid X receptor; GLP-1, glucagon-like peptide-1; GPBAR1, G protein–coupled bile acid receptor; IBMX, 3-isobutyl-1-methylxanthine; qRT-PCR, quantitative RT-PCR; RFP, red fluorescent protein; RYGB, Roux-en-Y gastric bypass; SGLT-1, sodium-dependent glucose transporter 1; TDCA, taurodeoxycholate; TLCA, taurolithocholate; YFP, yellow fluorescent protein.

rect contact with the gut lumen and can sense nutrients and other components within the gastrointestinal tract. L-cell sensory mechanisms include G protein–coupled receptors, nutrient transporters, and ion channels (3).

The properties of GLP-1 have been exploited for the treatment of type 2 diabetes via the use of GLP-1 mimetics and inhibitors of GLP-1 inactivation by dipeptidyl peptidase-4 (4). The glucose dependence of GLP-1–triggered insulin release results in a low incidence of hypoglycemic side effects with these treatments, and GLP-1 mimetics offer the additional benefit of promoting weight loss. Understanding the mechanisms underlying the release of endogenous GLP-1 may facilitate the development of novel therapeutic approaches that promote secretion of endogenous gut hormones, in theory providing enhanced effects compared to those of exogenous agonists while possibly avoiding side effects due to the natural site of release and action of the endogenous hormone. This theory is supported by the results of bariatric procedures such as Roux-en-Y gastric bypass (RYGB). After RYGB, glycemic control often improves within days and precedes significant weight loss (5). Alterations in gut hormone signaling, including ~10-fold elevations of GLP-1 and peptide YY concentrations, probably contribute to the observed improvement in insulin secretion and decreased appetite (6).

Bile acids are amphipathic, steroid-based molecules that aid the digestion of fat when released into the upper small intestine. Ninety-five percent of bile acids are reabsorbed in the lower small intestine by the apical sodium-dependent bile acid transporter (ASBT). Bile acids are detected by the nuclear farnesoid X receptor (FXR) (7) and the G protein–coupled bile acid receptor GPBAR1 (TGR5), a primarily $G\alpha_s$-coupled receptor that increases intracellular cAMP levels upon activation (8). In L-cells, GPBAR1 activation resulted in GLP-1 release. The receptor has also been reported to activate type 2 iodothyronine deiodinase and promote energy expenditure in other tissues (9). Plasma bile acid concentrations have been reported to increase after RYGB and have been hypothesized to contribute to the beneficial metabolic effects of surgery (10), although this does not explain the early postoperative improvements (11).

Numerous groups are attempting to design effective drugs to target GPBAR1 and thereby to stimulate endogenous GLP-1 release as a new treatment for diabetes. GPBAR1 agonists have been shown to increase GLP-1 secretion and lower blood glucose in animal models (9, 12), but toxic side effects on the gallbladder have been reported (13). It has therefore been suggested that nonabsorbable agents or agonists with very low systemic exposure might be capable of activating L-cells without causing toxic systemic levels (14), although this approach depends on a better understanding of how bile acids and GPBAR1 ligands access their receptors.

In this article, we investigated the actions of bile acids on primary L-cells and intact intestinal epithelium. Single-cell imaging revealed that bile acids elevate cAMP and Ca^{2+} in L-cells. We established a Ussing chamber system to measure GLP-1 release and showed that in both this model and the perfused intestine bile acids preferentially stimulate GLP-1 secretion when applied from the basolateral (vascular) direction. In the Ussing chamber setup, apically applied taurodeoxycholate (TDCA) was largely ineffective when administered after pretreatment with an inhibitor of the ASBT, and both TDCA and a GPBAR1 agonist were more effective when applied to the basolateral than to the apical surface. GLP-1 secretory responses to bile acids and the GPBAR1 agonist were abolished in tissues from GPBAR1-knockout mice. Our combined data suggest that bile acids target basolaterally located GPBAR1 on L-cells and that luminally applied GPBAR1 ligands are effective only after absorption across the epithelial layer.

Materials and Methods

Transgenic mice

All animal procedures were approved by local ethical review committees and conformed to relevant national guidelines. GLU-Venus mice were described previously (15). GCaMP3 was expressed in L-cells by crossing GLU-Cre (16) with ROSA26-tdRFP (17) and ROSA25-GCaMP3 (18) strains. The cAMP sensor Epac2camps (19, 20) was expressed in L-cells under proglucagon promoter control in GLU-Epac transgenic mice (21). All mice were backcrossed onto a C57B6 genetic background, and both sexes were used in approximately equal numbers. GPBAR1-knockout mice were described previously (9). These were imported from Lausanne to Cambridge for this study, and only males were used for this part of the study.

Primary murine intestinal cultures

Cultures were prepared as described previously from 2- to 5-month-old mice (15). Lower small intestinal cultures contained ~12 cm of tissue proximal to the ileocolic junction, with the exception of experiments involving GPBAR-knockout mouse tissue, for which regions up to 2 cm and between 7 and 15 cm proximal to the ileocolic junction were used. Tissue was digested with 0.3 to 0.4 mg/mL collagenase XI, centrifuged at 100 × *g*, and resuspended in DMEM (25 mmol/L glucose) supplemented with 10% (vol/vol) fetal bovine serum, 2 mmol/L L-glutamine, 100 U/mL penicillin, and 0.1 mg/mL streptomycin. Aliquots of tissue digests were plated and incubated at 37°C and 5% CO_2.

Primary murine intestinal single-cell suspension for fluorescence-activated cell sorting (FACS)

Tissue was digested in 1 mg/mL collagenase XI in calcium-free Hanks' buffered salt solution, centrifuged at 300 × *g*, re-

suspended in a low chloride (Cl^-) buffer (40 mmol/L sodium citrate, 75 mmol/L sodium acetate, 3.5 mmol/L KCl, 10 mmol/L HEPES, 4 mmol/L sodium hydrogen carbonate, and 5.5 mmol/L glucose [pH 7.4]), with 1% (wt/vol) fatty acid–free bovine serum albumin (BSA). Single cell suspensions were separated by flow cytometry using a MoFlo Beckman Coulter Cytomation sorter (Coulter Corp). Side scatter, forward scatter, and pulse-width gates excluded debris and aggregates. Venus-positive cells were collected alongside negative (control) cells (15) into lysis buffer for mRNA extraction.

RNA extraction and quantitative RT-PCR (qRT-PCR)

Total RNA from FACS-isolated cells and whole tissue segments was isolated using a micro scale RNA isolation kit (RNeasy; Qiagen) and TRI Reagent, respectively. Next, 200 to 350 ng of RNA was reverse-transcribed according to standard protocols using a Peltier Thermal Cycler PTC-225 (MJ Research). qRT-PCR was performed with a 7900 HT Fast Real-Time PCR system (Applied Biosystems). The PCR mix contained a first-strand cDNA template, primers (TaqMan gene expression assays; Applied Biosystems), and PCR Master Mix (Applied Biosystems). Expression was compared with that of β-actin measured on the same sample in parallel, giving a cycle threshold difference (ΔC_T) for β-actin minus the test gene. Mean, SEM, and statistics were obtained for the ΔC_T data and converted to relative expression levels ($2^{\Delta}C_T$) for presentation.

GLP-1 secretion assay

Secretion studies were performed ~20 hours after plating on 24-well culture plates coated with Matrigel (BD Biosciences). Cultures were incubated with test reagents in a standard saline solution (see below) containing 0.1% (wt/vol) fatty acid–free BSA, 10 mmol/L glucose and protease inhibitors (10 μmol/L amastatin hydrochloride, 100 μmol/L diprotin A, and 18 μmol/L aprotinin) for 2 hours at 37°C. Media were collected and centrifuged. Plated cells were mechanically disrupted in lysis buffer containing 50 mmol/L Tris-HCl, 150 mmol/L NaCl, 1% IGEPAL CA-630, 0.5% deoxycholic acid, and complete EDTA-free protease inhibitor cocktail (Roche) to extract intracellular peptides. GLP-1 was assayed in supernatants and cell extracts with a total GLP-1 assay (MesoScale Discovery). GLP-1 secretion in each well was expressed as a fraction of the total hormone measured in the same well.

Calcium imaging

Cultures were generated from GLU-Cre/ROSA26-tdRFP/ROSA25-GCaMP3 mice (22). An inverted fluorescence microscope (Olympus IX71) with a ×40 oil-immersion objective lens was used for signal visualization. GCaMP3 and red fluorescent protein (RFP) were excited at 488 nm and at 555 nm, respectively, using a monochromator (Cairn Research) and a 75-W xenon arc lamp, and GCaMP fluorescence was recorded using a 510-nm long-pass filter and an Orca ER camera (Hamamatsu). Images were collected using MetaFluor software (Molecular Devices). Solutions were perfused at ~1 mL/min. Mean fluorescence in the test agent was normalized to the mean basal fluorescence of each cell, measured before the addition and after washout of test compounds. Cells failing to exhibit a >1.1-fold change in GCaMP3 fluorescence to any stimuli, including the positive control, were excluded from analysis.

cAMP imaging

Cultures were generated from GLU-Epac mice, expressing the Förster resonance energy transfer–based sensor Epac2-camps (19–21). An inverted fluorescence microscope with a ×40 oil-immersion objective lens was used for signal visualization. Excitation at 435 nm was achieved using a 75-W xenon arc lamp coupled to a monochromator controlled by MetaFluor software. Cyan fluorescent protein (CFP) emission at 470 nm and yellow fluorescent protein (YFP) emission at 535 nm were monitored using an Optosplit II beam splitter (Cairn Research) and an Orca ER digital camera and are expressed as the CFP/YFP fluorescence ratio. Solutions were perfused at ~1 mL/min. Data were smoothened with a sliding average across 30 seconds. Maximum ratios were determined at baseline (30-second period before the test condition) and after test reagent application. Responses to test reagents are expressed relative to baseline levels.

Ussing chamber measurements

Mice were euthanized by cervical dislocation, and the whole length of the intestine was transported in ice-cold L-15 medium. The part of the ileum that was 2 to 7 cm proximal to the ileocecal connection was removed and divided into 4 segments, each ~1.25 cm long. Segments were cut longitudinally along the remnants of the mesenteric attachment and washed with Ringer solution containing 120 mmol/L NaCl, 3 mmol/L KCl, 0.5 mmol/L $MgCl_2$, 1.25 mmol/L $CaCl_2$, and 23 mmol/L $NaHCO_3$, with 10 mmol/L mannitol. Serosa and most of the muscular layer were stripped away with fine forceps. The segments were mounted in an Ussing chamber (EM-LVSYS-4 system with P2400 chambers and P2404 sliders; Physiologic Instruments). Up to 4 segments from each animal were used. The active epithelial surface area of each segment was 0.25 cm^2. Both parts of the Ussing chambers were filled with Ringer solution with added mannitol (10 mmol/L) apically and added glucose (10 mmol/L) basolaterally, maintained at 37°C, and continuously bubbled with 5% CO_2/95% O_2 (vol/vol). The transepithelial potential difference was continuously monitored under open circuit conditions, using a DVC 1000 amplifier (WPI) and recorded through Ag-AgCl electrodes and 150 mmol/L NaCl agarose bridges. Recordings were collected and stored using a Digidata 1440A acquisition system and AxoScope 10.4 software (both from Molecular Devices). First, transepithelial resistance and potential difference were allowed to stabilize for 20 to 30 minutes. During this period, transepithelial resistance was assessed by measuring voltage changes in response to 45-μA pulses lasting 2.5 seconds, applied every 100 seconds. After stabilization of the electrical parameters, solutions from both sides were removed. The apical sides of the chambers were refilled with 1.2 mL of fresh Ringer solution containing 10 mmol/L glucose, and the basolateral sides were filled with 1.2 mL of fresh Ringer solution containing 10 mmol/L glucose, 0.1% fatty acid–free BSA, 10 μmol/L amastatin, and 500 kIU/mL aprotinin. To prevent extensive foam formation, Infacol (Forest Laboratories) was added to the basolateral compartment ($1:10^5$ dilution). At 5 to 10 minutes after the solution exchange, samples (120 μL) were taken from the basolateral compartment and assayed for GLP-1 content as already described. Drugs were then applied as stated, and GLP-1 concentrations were measured typically 15, 60, and 90 minutes after the addition of stimulants. Fresh solution was added to replenish volumes lost by sampling. At the end of the experiment, forskolin

(10 μmol/L) and 3-isobutyl-1-methylxanthine (IBMX) (100 μmol/L) were added bilaterally to test the viability and tightness of the tissue. Preparations showing a <1 mV increase in the transepithelial potential difference (2 of 87) were excluded from further analysis. For each experimental protocol, numbers of tissue sheets were equal to the numbers of animals used. Reported GLP-1 secretion was normalized for 1 cm^2 of the tissue and a 60-minute secretion period.

Rat intestinal perfusion

Methods are described in more detail elsewhere (23). In brief, nonfasting male Wistar rats (~250 g) were anesthetized with fentanyl, fluanisone, and midazolam and placed on a 37°C heated table. The upper half of the small intestine and the entire large intestine were removed after the supplying vasculature was tied off. The remainder of the small intestine was cannulated and luminally perfused with isotonic saline at ~0.25 mL/min at room temperature. A catheter was placed in the cranial/superior mesenteric artery and perfused (7.5 mL/min) with modified Krebs-Ringer buffer gassed with 95% O_2 and 5% CO_2 (vol/vol) and warmed (37°C) by a Uniper UP-100 perfusion system (Hugo Sachs; Harvard Apparatus). The venous effluent was collected via a catheter in the hepatic portal vein. Once catheters were in place, rats were killed by perforation of the diaphragm and the system was allowed to equilibrate for 30 minutes. Intestines were stimulated luminally or vascularly by adding agents to the relevant perfusates. Luminal stimulations were applied at an initial rate of 2.5 mL/min for the first 2 minutes to replace the saline solution in the lumen and thereafter at 0.5 mL/min. Lumens were then flushed with a similar bolus of 0.9% NaCl (2.5 mL/min) for 2 minutes, followed by infusion at 0.250 mL/min between stimulations. Bombesin (BBS) (10 nmol/L vascularly) was included in all experiments as a positive control. Venous effluent was collected each minute, chilled on ice, and transferred to −20°C within 30 minutes. Effluent GLP-1 concentrations were measured using a total GLP-1 RIA as described previously (24).

Chemicals

The standard saline solution contained 138 mmol/L NaCl, 4.5 mmol/L KCl, 4.2 mmol/L $NaHCO_3$, 1.2 mmol/L NaH_2PO_4, 2.6 mmol/L $CaCl_2$, 1.2 mmol/L $MgCl_2$, and 10 mmol/L HEPES. The low Na^+ solution contained 138 mmol/L *N*-methyl-D-glucamine, 4.5 mmol/L KCl, 4.2 mmol/L $NaHCO_3$, 1.2 mmol/L NaH_2PO_4, 2.6 mmol/L $CaCl_2$, 1.2 mmol/L $MgCl_2$, and 10 mmol/L HEPES. Experiments involving a $CoCl_2$ solution contained 143.4 mmol/L NaCl, 4.5 mmol/L KCl, 2.6 mmol/L $CaCl_2$, 1.2 mmol/L $MgCl_2$, and 10 mmol/L HEPES, with or without the addition of 5 mmol/L $CoCl_2$. Rat perfusion buffer consisted of Krebs-Ringer bicarbonate buffer supplemented with 0.1% BSA, 5% dextran T-70 (Pharmacosmos), 3.5 mmol/L glucose, 10 μmol/L IBMX, and 5 mmol/L pyruvate, fumarate, and glutamate (pH 7.4).

Unless stated otherwise, all drugs and chemicals were obtained from Sigma-Aldrich. Forskolin and IBMX were dissolved in dimethyl sulfoxide (DMSO). Taurolithocholic acid was dissolved in methanol as a 100 mmol/L stock. Taurocholic acid and taurodeoxycholic acid stock solutions were 100 mmol/L, prepared in saline solution. Stocks (1000× of the GPBAR1 agonist, referred to as GPBAR-A [4-[[3,5 bis(trifluoromethyl)phenyl] methyl]-6-(2-fluorophenyl)-4,5-dihydro-pyrido[3,2-f]-1,4-oxazepin-3(2*H*)-one (25)] and GW4064 were prepared in DMSO at 3 and 5 mmol/L, respectively. The ASBT inhibitor (GSK2331583C) was obtained from GlaxoSmithKline and dissolved in DMSO (10 mmol/L). When DMSO was used as a solvent, the working concentration never exceeded 0.2% (vol/vol). Control studies confirmed that this concentration did not stimulate GLP-1 secretion (data not shown). Stock solutions of amastatin (10 mmol/L) and aprotinin (20 500 kIU/mL) were prepared in water.

Statistical analysis

Comparisons between conditions were made using one- or two-way ANOVAs and post hoc Bonferroni multiple comparison or Student *t* tests as indicated in the figure legends (GraphPad Prism), with a threshold for significance of $P = .05$.

Results

Bile acid–stimulated GLP-1 secretion from primary intestinal cultures

In primary murine intestinal cultures, bile acids dose dependently increased GLP-1 release (Figure 1). In both ileal and colonic cultures, TDCA was more effective than taurolithocholate (TLCA) or TCA, when compared at the same concentration (100 μmol/L). This order of potency differs from the reported responsiveness of GPBAR1, which prefers TLCA > TDCA > TCA (26). Consistent with the idea that bile acids act through GPBAR1, a GPBAR1 agonist (GPBAR-A) (8, 25) was also effective in stimulating GLP-1 secretion. The FXR agonist GW4064 (7) had little effect on GLP-1 release in intestinal cultures.

To ensure that the GLP-1 concentrations detected during secretion studies were not due to the cytotoxic effects of bile acids, a colorimetric lactate dehydrogenase assay (Pierce) was used. Very low levels of lactate dehydrogenase were detected in the extracellular medium (0.1%–0.5% total), and no correlation with the GLP-1 concentration was observed (data not shown).

Bile acid–induced intracellular cAMP and calcium changes

In considering the results of the secretion studies, it is possible that bile acids trigger both GPBAR1-dependent and -independent pathways in primary cultured L-cells. We therefore performed single-cell imaging studies to identify the intracellular signaling pathways activated by bile acids in L-cells. For this, we used transgenic mice which express fluorescent sensors for cAMP or Ca^{2+} specifically in L-cells. These enable real-time monitoring of these second messengers in response to a variety of stimuli.

First, we monitored cAMP changes using GLU-Epac mice that express the Förster resonance energy transfer–based cAMP sensor Epac2-camps in L-cells. Bile acids trig-

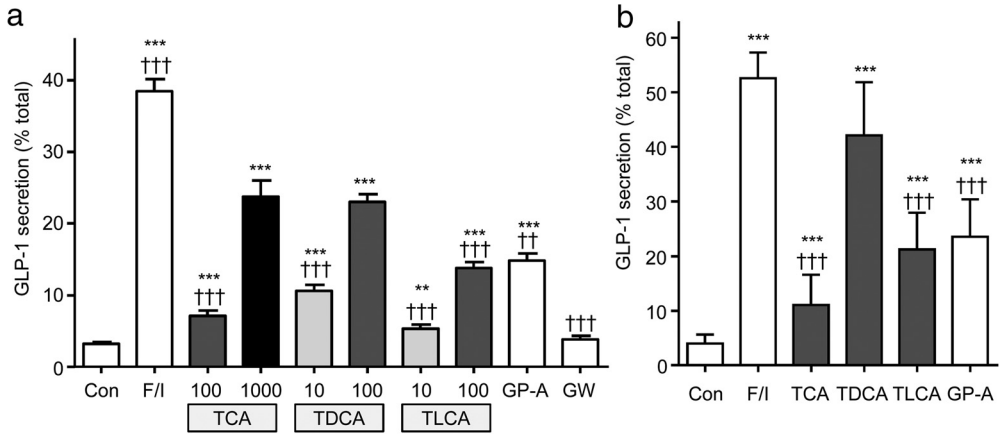

Figure 1. Bile acid–induced GLP-1 secretion. Small intestinal (A) or colonic (B) cultures were incubated for 2 hours in saline solution containing 10 mmol/L glucose (control [Con]) and the following stimuli at the concentrations indicated (μmol/L): F/I, forskolin (10 μmol/L) plus IBMX (10 μmol/L), TCA, TDCA, TLCA, GPBAR-A (GP-A) (3 μmol/L), and GW4064 (GW) (5 μmol/L). GLP-1 release is expressed as a percentage of content. The results are the means ± SEM of n = 12 to 23 wells (A) and n = 12 wells, all bile acids at 100 μmol/L (B), with 3 to 4 wells originating from a single mouse performed in parallel. Statistical differences were determined using a one-way ANOVA and a post hoc Bonferroni test on $\log_{10}$-transformed data. Statistical differences from basal (*) or TDCA at 100 μmol/L (†) are displayed: **/††, $P < .01$; ***/†††, $P < .001$.

gered robust elevation of cAMP (monitored as CFP/YFP) in ileal L-cells, as predicted, based on the known recruitment by GPBAR1 of $G\alpha_s$ proteins and activation of adenylate cyclase (Figure 2, A and B). TDCA (10 μmol/L and 100 μmol/L), TLCA (10 μmol/L and 100 μmol/L), and GPBAR-A (3 μmol/L) significantly increased the CFP/YFP ratio ($P < .05$ vs baseline), and no statistical differences were found between TDCA and TLCA.

Next we monitored Ca^{2+} in ileal L-cells using the sensor GCaMP3, expressed specifically in L-cells in the mouse

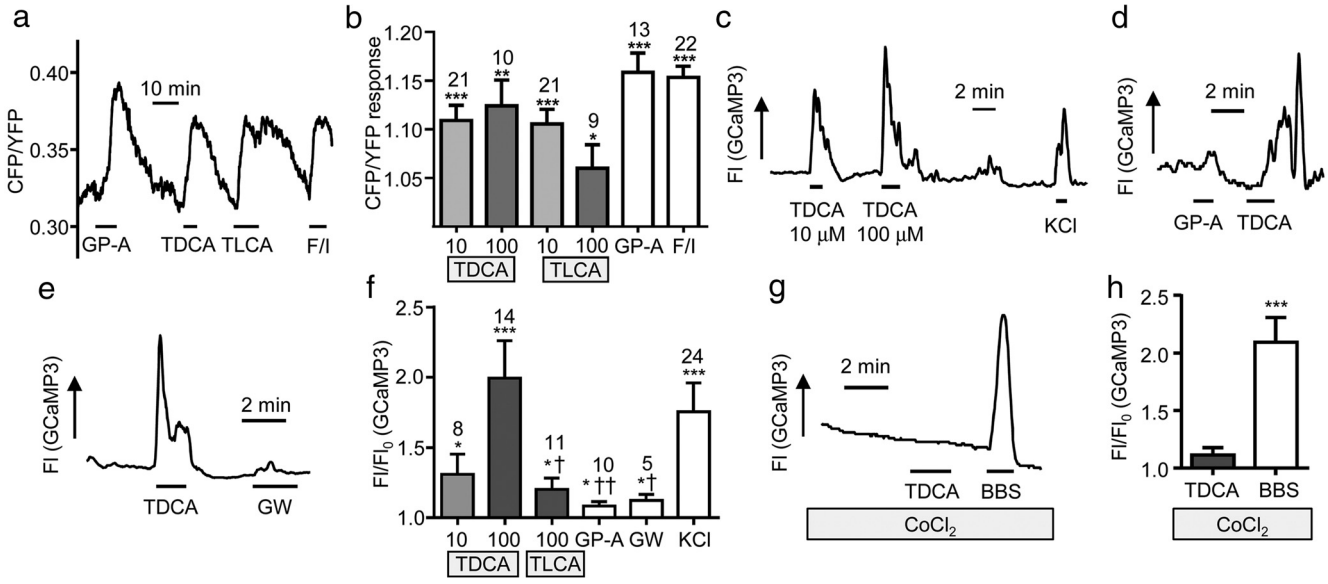

Figure 2. Intracellular cAMP and Ca^{2+} changes in L-cells. Mixed intestinal cultures were generated from the lower small intestine of mice expressing Epac2camps (A and B) or GCaMP3 (C and H) in L-cells. Cells were perfused with stimuli as indicated in saline buffer containing 10 mmol/L glucose. A, Representative cAMP response from an L-cell stimulated with GPBAR-A (GP-A; 3 μmol/L), TDCA (10 μmol/L), TLCA (10 μmol/L), and forskolin (10 μmol/L) plus IBMX (100 μmol/L) (F/I). B, Mean fold change in the CFP/YFP ratio, representing [cAMP], for cells recorded as in A. Error bars represent SEM; numbers of individual cells are indicated above the bars. Statistical differences from basal were determined by a one-sample *t* test (*, $P < .05$; **, $P < .01$; ***, $P < .001$). Bile acids were applied at 10 or 100 μmol/L as indicated. C–E, Representative L-cell calcium responses measured as GCaMP3 fluorescence (FI) to TDCA at the concentrations indicated and 30 mmol/L KCl (C), GPBAR-A (GP-A, 3 μmol/L), GW4064 (GW, 5 μmol/L), or TDCA (100 μmol/L) (D and E). F, Mean increase in GCaMP3 fluorescence over baseline (FI/FI_0) for cells recorded as in C to E. TLCA and TDCA concentrations were 10 or 100 μmol/L as indicated. Cells that did not respond to any stimuli were excluded from analysis (4 of 28). Results are means ± SEM, and numbers of individual cells are indicated above the bars. Statistical differences from basal signal (*) were determined via one-sample *t* tests and statistical differences from TDCA (†) were determined by a one-way ANOVA and post hoc Bonferroni test on $\log_{10}$-transformed data (*/†, $P < .05$; ††, $P < .01$; ***, $P < .001$). G and H, Cells were recorded and analyzed as in C–F, but in the presence of $CoCl_2$ (5 mmol/L) to block voltage-gated Ca^{2+} channels. BBS (100 nmol/L) was used as a positive control. Two of 14 cells were excluded. ***, $P < .001$ by a one-sample *t* test on $\log_{10}$-transformed data compared with basal.

strain GLU-Cre/ROSA26-GCaMP3. TDCA at 100 μmol/L triggered a rapid and reversible 1.7-fold increase in GCaMP3 fluorescent intensity, indicative of an elevation of intracellular Ca^{2+}. This was significantly greater than the responses observed with 100 μmol/L TLCA (1.2-fold increase, $P < .05$). The GPBAR1 agonist and the FXR agonist GW4064 triggered only small changes in GCaMP3 fluorescence (Figure 2, C–F). This pattern of Ca^{2+} responsiveness supports the idea that TDCA recruits an additional signaling pathway in L-cells, not related to activation of GPBAR1 or FXR. The effect of TDCA was significantly impaired in the presence of cobalt chloride ($CoCl_2$, 5 mmol/L), which blocks voltage-gated calcium channels, indicating that the Ca^{2+} rise was largely attributable to extracellular Ca^{2+} entry (Figure 2, G and H).

We hypothesized that TDCA transport might trigger membrane depolarization and V-gated Ca^{2+} entry as a consequence of electrogenic Na^+-coupled influx by the ASBT, analogous to our previous findings with sodium-dependent glucose transporter 1 (SGLT1) (16, 23). Indeed, *Asbt* was detected in ileal and colonic L-cells by qRT-PCR (Figure 3, A and B). When extracellular Na^+ was reduced ~25-fold to 5.6 mmol/L, however, TDCA still elicited an elevation of intracellular Ca^{2+} in L-cells (Figure 3, C and D). To test the role of ASBT directly, we used a specific ASBT inhibitor (10 μmol/L) in GLP-1 secretion and calcium imaging experiments. The inhibitor did not significantly impair TDCA-triggered GLP-1 release or Ca^{2+} responses in cell cultures, suggesting that TDCA-induced GLP-1 secretion is not directly coupled to bile acid uptake by L-cells via ASBT (Figure 3, E–G).

Role of bile acid uptake

To assess GLP-1 secretion from intact intestinal tissue pieces, we adapted the use of Ussing chambers, in which epithelial integrity is maintained and test agents can be

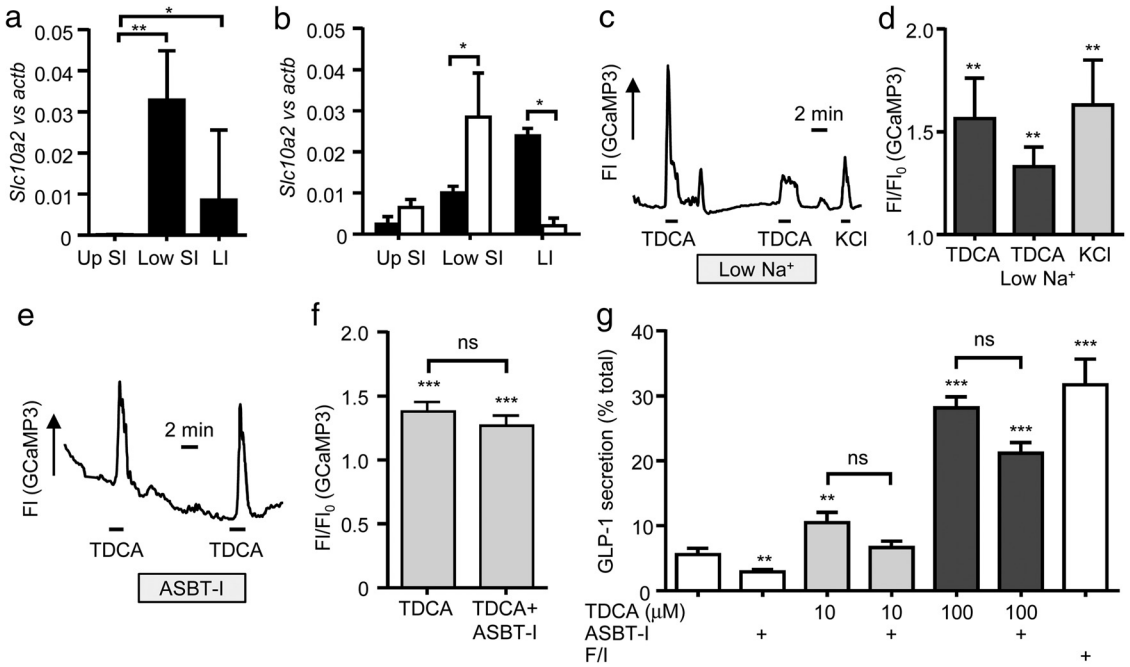

Figure 3. The role of ASBT in bile acid–induced GLP-1 release and intracellular Ca^{2+} changes. Expression of *Asbt* was determined in homogenized intestine segments (A) and FACS-isolated L-cell populations (B). Expression of *Asbt* (Slc10a2) in control cells (□) and L-cells (■) was determined relative to that of β-actin by qRT-PCR. Up SI, upper 10 cm of the small intestine; low SI, lower 12 cm of the small intestine; LI, large intestine. Mean ΔC_T and upper SEM were calculated from 3 independent experiments and are presented as $2^{\Delta}C_T$. Statistical tests were assessed on nontransformed data using a one-way ANOVA and post hoc Bonferroni test (A) or two-tailed *t* tests (B) (*, $P < .05$; **, $P < .01$). C–F, Mixed lower small intestinal cultures of mice expressing GCaMP3 in L-cells were perfused with standard saline containing 10 mmol/L glucose and additions as indicated. C, Representative trace depicting GCaMP3 fluorescence (FI) in response to TDCA (100 μmol/L) applied in standard and low (5.6 mmol/L) Na^+ saline and 30 mmol/L KCl. D, Mean increase in GCaMP3 fluorescence over baseline (FI/FI_0) for cells recorded as in C. Cells that did not respond to any stimuli (all responses <1.1-fold) were excluded (2 of 14). Results are means ± SEM (n = 12). Statistical significance from basal was determined on $\log_{10}$-transformed data via a one-sample *t* test (**, $P < .01$). E, Representative trace depicting a calcium response to TDCA (10 μmol/L) with and without the ASBT inhibitor (ASBT-I; 10 μmol/L). F, Mean ± SEM data are recorded as in E (n = 4). Statistical analysis was performed as in D (***, $P < .001$ from basal). G, Lower small intestinal cultures were incubated for 2 hours in saline solution containing 10 mmol/L glucose and stimuli as indicated. Test agents were TDCA (100 mymol/L), ASBT-I (10 μmol/L), and 10 μmol/L forskolin plus 10 μmol/L IBMX (F/I). GLP-1 release is expressed as a percentage of content. Results are means ± SEM of n = 12 wells, with 4 wells originating from a single mouse performed in parallel. Statistical differences were determined using a one-way ANOVA and post hoc Bonferroni test on $\log_{10}$-transformed data (**, $P < .01$; ***, $P < .001$, compared with basal).

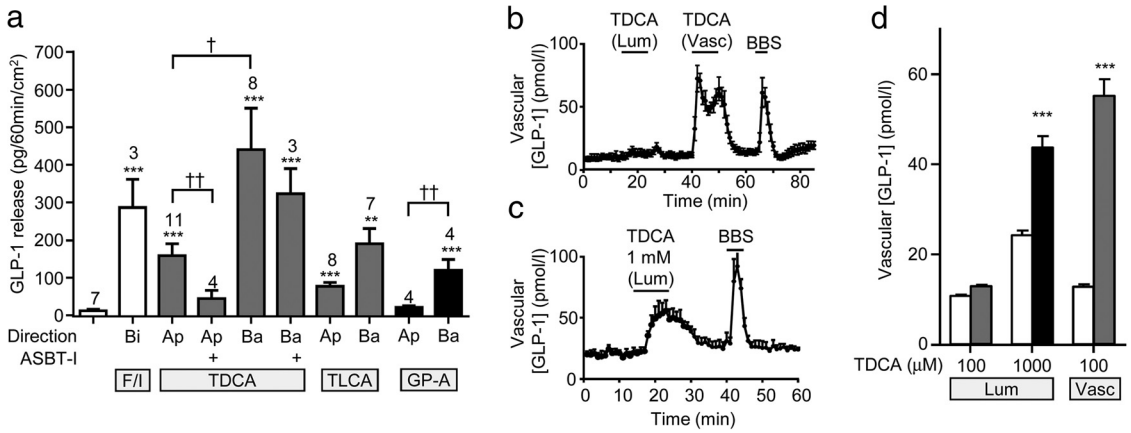

Figure 4. GLP-1 secretion from murine ileal epithelial tissues mounted in Ussing chambers and from perfused rat intestine. A, Concentration change in GLP-1 in the basolateral compartment of Ussing chambers was assessed after 1 hour without treatment (left-hand column) or with treatment with TDCA (100 μmol/L), TLCA (100 μmol/L), GPBAR-A (GP-A; 3 μmol/L), or forskolin (10 μmol/L) plus IBMX (100 μmol/L) (F/I), applied to the apical (Ap), basolateral (Ba), or both compartments (bilaterally [Bi]) as indicated. At 10 minutes before application of TDCA, some tissues were pretreated bilaterally with 10 μmol/L ASBT inhibitor (ASBT-I). Results are normalized per 1 cm^2 tissue area. Means ± SEM and numbers of tissue sheets are indicated. Statistical differences were determined on $\log_{10}$-transformed data using a one-way ANOVA and post hoc Bonferroni test either from basal (*) or between conditions as indicated (†) (†, $P < .05$; **/††, $P < .01$; ***, $P < .001$). B–D, TDCA-stimulated GLP-1 secretion from perfused rat intestine. B, TDCA (100 μmol/L) was applied to either the luminal (Lum) or vascular (Vasc) side. C, TDCA (1 mmol/L) was applied to the luminal side. BBS (10 nmol/L, vascular) was included at the end of all experiments as a positive control. Meas ± SEM GLP-1 responses from n = 6 to 7 perfused rat intestines (B and C) and time-averaged GLP-1 levels at baseline (□) and during TDCA addition (▨, 100 μmol/L/■, 1 mmol/L) (D) for experiments performed as in B and C are shown. Statistical differences from basal (*) were determined by a one-way ANOVA and post hoc Bonferroni test (***, $P < .001$).

applied independently to the luminal or basolateral compartments. In validation experiments on sheets of terminal ileum, bilateral addition of forskolin plus IBMX elicited a robust GLP-1 secretory response into the basolateral compartment of the chambers (Figure 4A).

When TDCA (100 μmol/L) or TLCA (100 μmol/L) was applied to either the apical or basolateral compartment, GLP-1 release was elevated compared with that for controls (Figure 4A). For both bile acids, basolaterally stimulated GLP-1 release was greater than that when they were applied

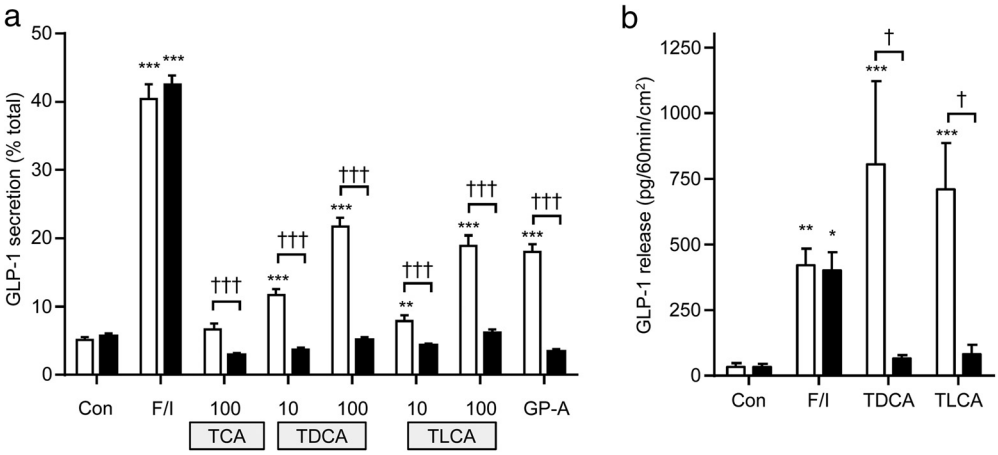

Figure 5. Bile acid–induced GLP-1 secretion from GPBAR-knockout mice. GLP-1 secretion was measured from small intestinal cultures or tissue sections from wild-type (□) and GPBAR-knockout (■) mice. A, Cultures were incubated for 2 hours in saline solution containing 10 mmol/L glucose (control [Con]) and the following stimuli at the concentrations indicated (μmol/L): F/I, forskolin (10 μmol/L) plus IBMX (10 μmol/L), TCA, TDCA, TLCA, and GPBAR-A (GP-A) (3 μmol/L). GLP-1 release is expressed as a percentage of content. Results are means ± SEM of n = 9 wells, with 3 wells originating from a single mouse performed in parallel. B, Concentration change in GLP-1 in the basolateral compartment of Ussing chambers was assessed after 1 hour without treatment or with treatment with TDCA (100 μmol/L), TLCA (100 μmol/L), applied to the basolateral compartment, or forskolin (10 μmol/L) plus IBMX (100 μmol/L) (F/I), applied bilaterally. Results are normalized per 1 cm^2 tissue area. Data are means ± SEM (n = 3–4). Statistical differences were determined using a two-way ANOVA and post hoc Bonferroni test on $\log_{10}$-transformed data. Statistical elevations from control (*) or differences between wild-type and knockout (†) mice are displayed: */†, $P < .05$; **, $P < .01$; ***/†††, $P < .001$.

apically, although this difference reached statistical significance only for TDCA (Figure 4A, $P < .05$). Bilateral application of the ASBT inhibitor largely abolished secretion triggered by subsequent apical TDCA but did not impair the responses to basolateral TDCA (Figure 4A). This result suggested that TDCA stimulated GLP-1 secretion after its ASBT-dependent transport from the apical to the basolateral compartment but did not require ASBT-dependent uptake by L-cells themselves. Application of GPBAR-A from the basolateral but not the apical direction also increased GLP-1 release (Figure 4A), suggesting a role for basolaterally located GPBAR1 on L-cells.

To validate the Ussing chamber method, we performed comparative experiments in the perfused rat intestinal model. In support of the findings from the Ussing chambers, application of 100 μmol/L TDCA via the vasculature robustly and reversibly increased GLP-1 release. Luminal application of the same TDCA concentration was largely ineffective (Figure 4, B and D), whereas 1 mmol/L TDCA stimulated GLP-1 secretion (1 mmol/L TDCA was not tolerated when applied via the vasculature, Figure 4C).

Role of GPBAR1

To assess the extent to which GPBAR1 is responsible for bile acid–stimulated GLP-1 release from L-cells, we measured GLP-1 secretion from GPBAR1-knockout mouse intestinal cultures and Ussing chamber-mounted tissue sections (Figure 5). TDCA, TCA, and TLCA did not significantly increase GLP-1 secretion above basal levels in primary intestinal cultures generated from GPBAR1-knockout mice (Figure 5A). In cultures from matched wild-type controls, GLP-1 levels were increased by bile acids and the GPBAR agonist (GPABAR-A) and were significantly greater than in cultures from GPBAR1-knockout animals for these agents ($P < .001$; Figure 5A). Similarly, TDCA and TLCA did not significantly stimulate GLP-1 secretion from GPBAR-knockout intestinal tissue sections mounted in Ussing chambers when applied to the basolateral compartment, whereas both bile acids triggered robust GLP-1 secretory responses in tissues from matched wild-type mice ($P < .05$; Figure 5B). No differences were observed for forskolin/IBMX-stimulated GLP-1 secretion between wild-type and knockout derived tissues in primary cultures or Ussing chambers (Figure 5). These data indicate that GPBAR1 is essential for mediating bile acid–stimulated GLP-1 release from L-cells.

Discussion

In this study, we investigated the effects of bile acids on L-cell function using a variety of techniques ranging from single cell imaging to measurements of GLP-1 release from the perfused intact gut. We also optimized and evaluated small-volume Ussing chambers as a technique for directly measuring gut hormone release from intact sheets of intestine. Our system generated GLP-1 concentrations, falling reliably within the working range of available immunoassays, even under basal (unstimulated) conditions, in contrast to previous reports using a similar approach (27). The method also differs from previous Ussing chamber studies that used changes in the short circuit current as a surrogate for hormonal release (28) and evaluation of the directionality of action of GPR119 agonists (29). Overall, our results indicate that bile acids trigger elevation of cAMP and Ca^{2+} in L-cells, but that the predominant link between luminal bile acids and GLP-1 release is probably mediated by GPBAR1 located on the basolateral L-cell membrane.

Consistent with the known coupling of GPBAR1 to $G\alpha_s$ proteins and activation of adenylate cyclase (26), bile acids increased cAMP concentrations in primary cultured L-cells. In addition, however, we found that TDCA substantially elevated L-cell intracellular Ca^{2+}. This latter effect was not mimicked by ligands of GPBAR1 or FXR and involved Ca^{2+} entry through plasma membrane calcium channels, suggesting that it might occur downstream of membrane depolarization. We hypothesized that this Ca^{2+} signal might be linked to bile acid uptake by ASBT, which cotransports at least 2 Na^+ ions for each bile acid molecule (30). If electrogenic ion transport occurs at a sufficient rate, it can lead to membrane depolarization, as reported previously for the SGLT1 (31). A highly selective ASBT inhibitor did not, however, impair TDCA-triggered GLP-1 secretion from primary cultures. Surprisingly, the ASBT inhibitor induced a small but significant reduction in basal GLP-1 release, suggesting that ASBT has intrinsic activity in L-cells even in the absence of added bile acids. Consistent with this idea, when ASBT was expressed in *Xenopus* oocytes, a bile-acid independent background current was reported (32). However, the lack of effect of the ASBT inhibitor on TDCA-triggered Ca^{2+} signals in L-cells indicated that an alternative mechanism is likely to underlie these responses. Bile acids have been reported to increase Ca^{2+} in a number of cell types, via mechanisms not yet identified at the molecular level (33). We searched our microarray transcriptomic database (34) for previously reported bile acid–sensitive proteins expressed in L-cells, but no convincing candidates were identified. ASIC5 has been reported to behave as a bile acid-activated amiloride-sensitive ion channel in some species (35) and was detected by microarray in L-cells, but seems not to underlie the Ca^{2+} responses in L-cells, as amiloride did not prevent the Ca^{2+} signal triggered by TDCA (data not

shown). Our data do not therefore allow us to draw conclusions about the molecular mechanisms underlying TDCA-triggered Ca^{2+} responses in L-cells. Although further calcium imaging experiments on GPBAR1-knockout tissues could address the requirement of GPBAR1 for this response, it appears that a putative GPBAR1-independent rise in cytosolic Ca^{2+} would be insufficient to stimulate a secretory response.

Our data from the perfused intestine and Ussing chambers suggest that the predominant effect of bile acids on GLP-1 release in intact tissue is triggered by GPBAR1 activation on the basolateral L-cell membrane. Findings in support of this idea are that basolaterally applied TDCA was more effective than apical TDCA in the perfused intestine and Ussing chamber system, that the ASBT inhibitor blocked apical TDCA-triggered but not basolateral TDCA-triggered GLP-1 release in Ussing chambers, that GPBAR agonist was effective only when applied to the basolateral compartment of Ussing chambers, and that bile acids did not stimulate GLP-1 secretion from GPBAR1-knockout mouse tissue. The location of GPBAR1 on L-cells has previously been difficult to pinpoint by immunomicroscopy, but a previous study also found that a nonabsorbable GPBAR1 agonist only triggered GLP-1 release when administered systemically, suggesting that the receptor is accessible from the basolateral but not the apical intestinal compartment (12). This is a critical issue for the field of therapeutic GPBAR1 agonist development. Previous reports that GPBAR1 agonists exhibited gallbladder toxicity in animal models (13) led to the suggestion that nonabsorbable GPBAR1 ligands or agonists with low systemic exposure might be required to target L-cells without triggering systemic side effects. Our data, however, suggest that luminally restricted agents would not elicit a strong GLP-1 secretory response in vivo.

Although bile acids are widely believed to play important roles in metabolism and to mediate beneficial effects after gastric bypass surgery (7, 10), published data on the effects of bile acid sequestrants and ASBT inhibitors on GLP-1 secretion have been inconclusive. The bile acid sequestrant, colesevelam, for example, acutely increased postprandial GLP-1 levels in humans, but the effect was not sustained at 4 weeks (36). Two weeks of treatment with an ASBT inhibitor, in contrast, resulted in persistently enhanced GLP-1 levels in rats (37). Our finding that bile acids predominantly act from the basolateral compartment offers some clarity to this field. On the one hand, treatment with sequestrants or ASBT inhibitors increases the delivery of nonabsorbed bile acids to the large intestine, with its dense L-cell population. In the colon, bile acids are modified by microbiota, and the resultant unconjugated secondary bile acids are absorbed passively (38). Increased colonic bile acid delivery could therefore result in increased bile acid concentrations in the basolateral compartment surrounding colonic L-cells and GPBAR1-dependent GLP-1 release. On the other hand, the aim of long-term administration of bile acid sequestrants and ASBT inhibitors is to deplete the plasma bile acid pool and tends to counteract some of this effect.

In summary, we find that bile acids trigger a variety of signaling pathways in L-cells, but it seems that GLP-1 release is largely determined by GPBAR1 activation. The location of functional GPBAR1 appears to be mostly basolateral on L-cells, requiring an initial step involving absorption across the intestinal epithelium before bile acids or GPBAR1 agonists can trigger GLP-1 secretion. This requirement for systemic availability of GPBAR1 ligands will make it difficult to harness this receptor therapeutically because of the reported gallbladder toxicity of systemically available agonists. Increasing delivery of bile acids to the distal gut by bariatric surgical procedures, resins, or ASBT inhibitors might, however, offer effective strategies to elevate concentrations of GPBAR1 ligands in the local vicinity of colonic L-cells.

Acknowledgments

The mesoscale GLP-1 immunoassays were performed by Keith Burling and colleagues at the Medical Research Council Metabolic Diseases Unit, Cambridge. The Ussing chamber equipment was initially kindly lent by Dr Todd Alexander, Departments of Pediatrics and Physiology, University of Alberta, Canada.

Address all correspondence and requests for reprints to: Fiona M. Gribble or Frank Reimann, Metabolic Research Laboratories and Medical Research Council Metabolic Diseases Unit, Wellcome Trust-Medical Research Council Institute of Metabolic Science, Addenbrooke's Hospital, Cambridge, CB2 0QQ, UK. E-mail: fmg23@cam.ac.uk or fr222@cam.ac.uk.

C.A.B., J.R., R.E.K., and L.L.G. performed and analyzed experiments. J.J.H., F.M.G., and F.R. designed the study and wrote the manuscript. K.S. provided the $GPBAR^{-/-}$ and $GPBAR^{+/+}$ control mice. All authors edited the final version of the manuscript.

This work was supported by the Wellcome Trust (Grants 084210/Z/07/Z, 088357/Z/09/Z, and 099825/Z/12/Z) and the Medical Research Council (Grant MRC_MC_UU_12012/3), the Novo Nordisk Center for Basic Metabolic Research (Novo Nordisk Foundation, Denmark), and the European Union's Seventh Framework Programme for Research, Technological Development, and Demonstration Activities (Grant 266408) J.R. was supported by an European Foundation for the Study of Diabetes Albert Renold Travel Fellowship. The laboratory of K.S. receives funding from the Swiss National Science Foundation (SNF 31003A_125487).

Disclosure Summary: The authors have nothing to disclose.

References

1. **Baggio LL, Drucker DJ.** Biology of incretins: GLP-1 and GIP. *Gastroenterology*. 2007;132:2131–2157.
2. **Holst JJ.** The physiology of glucagon-like peptide 1. *Physiol Rev*. 2007;87:1409–1439.
3. **Tolhurst G, Reimann F, Gribble FM.** Intestinal sensing of nutrients. *Handb Exp Pharmacol*. 2012;209:309–335.
4. **Nauck MA.** Incretin-based therapies for type 2 diabetes mellitus: properties, functions, and clinical implications. *Am J Med*. 2011; 124(1 Suppl):S3–S18.
5. **Jørgensen NB, Jacobsen SH, Dirksen C, et al.** Acute and long-term effects of Roux-en-Y gastric bypass on glucose metabolism in subjects with type 2 diabetes and normal glucose tolerance. *Am J Physiol Endocrinol Metab*. 2012;303:E122–E131.
6. **Jørgensen NB, Dirksen C, Bojsen-Møller KN, et al.** Exaggerated glucagon-like peptide 1 response is important for improved β-cell function and glucose tolerance after Roux-en-Y gastric bypass in patients with type 2 diabetes. *Diabetes*. 2013;62:3044–3052.
7. **Lefebvre P, Cariou B, Lien F, Kuipers F, Staels B.** Role of bile acids and bile acid receptors in metabolic regulation. *Physiol Rev*. 2009; 89:147–191.
8. **Parker HE, Wallis K, le Roux CW, Wong KY, Reimann F, Gribble FM.** Molecular mechanisms underlying bile acid-stimulated glucagon-like peptide-1 secretion. *Br J Pharmacol*. 2012;165:414–423.
9. **Thomas C, Gioiello A, Noriega L, Strehle A, Oury J, Rizzo G, et al.** TGR5-mediated bile acid sensing controls glucose homeostasis. *Cell Metab*. 2009;10:167–177.
10. **Patti ME, Houten SM, Bianco AC, et al.** Serum bile acids are higher in humans with prior gastric bypass: potential contribution to improved glucose and lipid metabolism. *Obesity (Silver Spring)*. 2009; 17:1671–1677.
11. **Jørgensen NB, Dirksen C, Bojsen-Møller KN, et al.** Improvements in glucose metabolism early after gastric bypass surgery are not explained by increases in total bile acids and fibroblast growth factor 19 concentrations. *J Clin Endocrinol Metab*. 2015;100:E396–E406.
12. **Ullmer C, Alvarez Sanchez R, Sprecher U, et al.** Systemic bile acid sensing by G protein-coupled bile acid receptor 1 (GPBAR1) promotes PYY and GLP-1 release. *Br J Pharmacol*. 2013;169:671–684.
13. **Li T, Holmstrom SR, Kir S, et al.** The G protein-coupled bile acid receptor, TGR5, stimulates gallbladder filling. *Mol Endocrinol*. 2011;25:1066–1071.
14. **Duan H, Ning M, Zou Q, et al.** Discovery of intestinal targeted TGR5 agonists for the treatment of type 2 diabetes. *J Med Chem*. 2015;58:3315–3328.
15. **Reimann F, Habib AM, Tolhurst G, Parker HE, Rogers GJ, Gribble FM.** Glucose sensing in L cells: a primary cell study. *Cell Metab*. 2008;8:532–539.
16. **Parker HE, Adriaenssens A, Rogers G, et al.** Predominant role of active versus facilitative glucose transport for glucagon-like peptide-1 secretion. *Diabetologia*. 2012;55:2445–2455.
17. **Luche H, Weber O, Nageswara Rao T, Blum C, Fehling HJ.** Faithful activation of an extra-bright red fluorescent protein in "knock-in" Cre-reporter mice ideally suited for lineage tracing studies. *Eur J Immunol*. 2007;37:43–53.
18. **Zariwala HA, Borghuis BG, Hoogland TM, et al.** A Cre-dependent GCaMP3 reporter mouse for neuronal imaging in vivo. *J Neurosci*. 2012;32:3131–3141.
19. **Nikolaev VO, Bünemann M, Hein L, Hannawacker A, Lohse MJ.** Novel single chain cAMP sensors for receptor-induced signal propagation. *J Biol Chem*. 2004;279:37215–37218.
20. **Friedlander R, Moss C, Mace J, et al.** Role of phosphodiesterase and adenylate cyclase isozymes in murine colonic glucagon-like peptide 1 secreting cells. *Br J Pharmacol*. 2011;163:261–271.
21. **Psichas A, Glass LL, Reimann F, Gribble FM.** Galanin inhibits GLP-1 and GIP secretion via the GAL1 receptor in enteroendocrine L and K cells. 2015.
22. **Emery EC, Diakogiannaki E, Gentry C, et al.** Stimulation of GLP-1 secretion downstream of the ligand-gated ion channel TRPA1. *Diabetes*. 2015;64:1202–1210.
23. **Kuhre RE, Frost CR, Svendsen B, Holst JJ.** Molecular mechanisms of glucose-stimulated GLP-1 secretion from perfused rat small intestine. *Diabetes*. 2015;64:370–382.
24. **Orskov C, Jeppesen J, Madsbad S, Holst JJ.** Proglucagon products in plasma of noninsulin-dependent diabetics and nondiabetic controls in the fasting state and after oral glucose and intravenous arginine. *J Clin Invest*. 1991;87:415–423.
25. **Keitel V, Cupisti K, Ullmer C, Knoefel WT, Kubitz R, Häussinger D.** The membrane-bound bile acid receptor TGR5 is localized in the epithelium of human gallbladders. *Hepatology*. 2009;50:861–870.
26. **Kawamata Y, Fujii R, Hosoya M, et al.** A G protein-coupled receptor responsive to bile acids. *J Biol Chem*. 2003;278:9435–9440.
27. **Geraedts MC, Takahashi T, Vigues S, et al.** Transformation of postingestive glucose responses after deletion of sweet taste receptor subunits or gastric bypass surgery. *Am J Physiol Endocrinol Metab*. 2012;303:E464–E474.
28. **Joshi S, Tough IR, Cox HM.** Endogenous PYY and GLP-1 mediate l-glutamine responses in intestinal mucosa. *Br J Pharmacol*. 2013; 170:1092–1101.
29. **Patel S, Mace OJ, Tough IR, et al.** Gastrointestinal hormonal responses on GPR119 activation in lean and diseased rodent models of type 2 diabetes. *Int J Obes (Lond)*. 2014;38:1365–1373.
30. **Zhou X, Levin EJ, Pan Y, et al.** Structural basis of the alternating-access mechanism in a bile acid transporter. *Nature*. 2014;505:569–573.
31. **Gribble FM, Williams L, Simpson AK, Reimann F.** A novel glucose-sensing mechanism contributing to glucagon-like peptide-1 secretion from the GLUTag cell line. *Diabetes*. 2003;52:1147–1154.
32. **Sun AQ, Balasubramaniyan N, Chen H, Shahid M, Suchy FJ.** Identification of functionally relevant residues of the rat ileal apical sodium-dependent bile acid cotransporter. *J Biol Chem*. 2006;281: 16410–16418.
33. **Voronina S, Longbottom R, Sutton R, Petersen OH, Tepikin A.** Bile acids induce calcium signals in mouse pancreatic acinar cells: implications for bile-induced pancreatic pathology. *J Physiol*. 2002; 540(Pt 1):49–55.
34. **Habib AM, Richards P, Cairns LS, et al.** Overlap of endocrine hormone expression in the mouse intestine revealed by transcriptional profiling and flow cytometry. *Endocrinology*. 2012;153:3054–3065.
35. **Lefèvre CM, Diakov A, Haerteis S, Korbmacher C, Gründer S, Wiemuth D.** Pharmacological and electrophysiological characterization of the human bile acid-sensitive ion channel (hBASIC). *Pflugers Arch*. 2014;466:253–263.
36. **Garg SK, Ritchie PJ, Moser EG, Snell-Bergeon JK, Freson BJ, Hazenfield RM.** Effects of colesevelam on LDL-C, A1c and GLP-1 levels in patients with type 1 diabetes: a pilot randomized double-blind trial. *Diabetes Obes Metab*. 2011;13:137–143.
37. **Chen LH, McNulty J, Anderson D, et al.** Cholestyramine reverses hyperglycemia and enhances glucose-stimulated glucagon-like peptide 1 release in Zucker diabetic fatty rats. *J Pharmacol Exp Ther*. 2010;334:164–170.
38. **Mekhjian HS, Phillips SF, Hofmann AF.** Colonic absorption of unconjugated bile acids: perfusion studies in man. *Dig Dis Sci*. 1979; 24:545–550.